THE JOURNAL OF PHYSICAL CHEMISTRY B

Article

pubs.acs.org/JPCB

Effect of Carbon Spacer Length on Zwitterionic Carboxybetaines

Qing Shao and Shaoyi Jiang*

Department of Chemical Engineering, University of Washington, Seattle, Washington 98195, United States

Supporting Information

ABSTRACT: Zwitterionic carboxybetaines (CBs) are ubiquitous in nature and considered promising materials for biological and chemical applications. A thorough understanding of the effect of carbon spacer length (CSL) on molecular properties is important. In this work, using molecular dynamics simulation and quantum chemical calculation, we investigated the effect of CSL on the molecular properties of CB molecules. The hydration number, structure, and dynamics of carboxylic and trimethyl ammonium groups were investigated and found to present different behaviors in regards to the variation of CSL. The simulation results with partial charges developed from quantum chemical calculations were compared with those with partial charges from the OPLS all atom (OPLSAA) force field. The hydration free energy of CB molecules and CB−Na^+ association was also studied as a function of CSL.

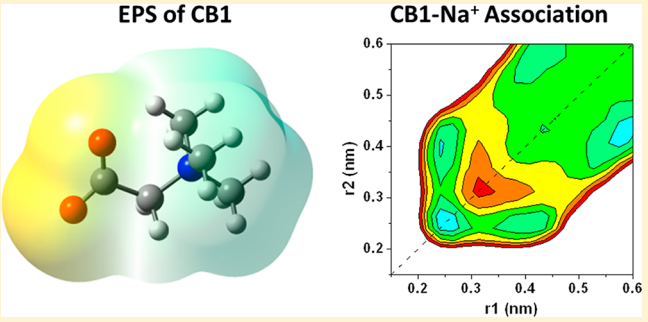

1. INTRODUCTION

Zwitterionic carboxybetaines (CBs) have received increasing attraction because of their importance in nature and their chemical and biological applications. In nature, glycine betaine and β-alanine betaine act as naturally occurring osmolytes and protein protectants.[1,2] Recent experiments have shown CB-based materials to be excellent candidates for applications such as drug delivery,[3] gene delivery,[4] and protein conjugation[5] because of their excellent resistance to nonspecific protein adsorption, biocompatibility, and versatility.[6] Understanding the structure−property relationship is critically important for not only the role of CB molecules in nature but also the development of applications based on them. A typical CB molecule is composed of a cationic trimethyl ammonium group and an anionic carboxylic group that are linked by methylene groups. The two charged groups are considered to be important for the properties of the CB molecules, and their distance can be altered by varying the number of methylene groups, which is called carbon spacer length (CSL).

The effect of CSL on zwitterionic molecules has been studied[7,8] in several experiments. For instance, Zhang et al.[9] investigated the protein adsorption of materials based on CBs with CSLs of one, two, three, and five methylene groups. Experiments showed that the CBs with various CSLs can all resist nonspecific protein adsorption but have different applicable pH scales. Vaisocherova et al.[10] further showed that only materials derived from CBs with CSLs of one and two methylene groups are able to resist nonspecific protein adsorption from 100% blood serum, while CBs with CSLs of three or more methylene groups cannot resist protein adsorption from this complex medium. More recently, Mi et al.[11] showed different binding behaviors of divalent cations for CB-based materials with different CSLs, leading to different interactions with polysaccharides outside bacteria. The effect of CSL on the other properties of materials has also been studied, including adsorbed protein conformation,[12] mobility of ionic group,[13] thermal stability of the material,[14] adsorption at the air−water interface,[15] and electroosmotic flow.[16] These observations offer solid proofs about the important roles of CSL.

Weers et al.[7] have studied how the solution properties of betaine surfactant varies with CSL, and their research showed the relationship between several properties of CB molecules and CSL. For instance, they showed that the pK_a of the molecule increases as the CSL increases. They also showed that the molecular dipole increases monotonically with the increase in CSL and suggested that there is probably no intramolecular association for charged groups. The critical micelle concentration was also found to be affected by the CSL.

However, the effect of CSL on the properties of CB molecules is poorly understood. One is its effect on hydration. Hydration is recognized to play an important role for applications in an aqueous environment.[3,17,18] It is well-known from studies of surfactants and lipids that the variation of alkyl chain length can change the ratio of hydrophobicity/hydrophilicity of a molecule[19,20] and thus the hydration. However, the variation of CSL brings more effects on the CB molecule than just alternating its hydrophobicity/hydrophilicity ratio. It could change the interplay of charged groups and the overlap of their coordination shells. The variation of these two factors can affect basic molecular hydration. Therefore, a thorough study of how the hydration of a CB molecule varies as

Received: September 23, 2012
Revised: January 12, 2013
Published: January 14, 2013

   dx.doi.org/10.1021/jp3094534 | J. Phys. Chem. B 2013, 117, 1357−1366

a function of CSL can not only offer insight in the hydration−structure relationship for a zwitterionic molecule but also guide the rational design of CB-based materials. Another critical effect of CSL regards the ionic association of the CB molecule. Previous studies have shown the important role of ionic association to the performance of zwitterionic materials.[21−23] Since the charges of charged groups are expected to vary with the variation of CSL, this may cause the variation of ionic association, which has not been thoroughly studied yet.

To address these issues, we will study the effect of CSL on the properties of CB molecules, focusing on hydration and ionic association. We will investigate hydration and ionic association from structural, dynamic, and energy aspects. The electron density distributions of CB molecules with various CSLs will also be investigated. The corresponding properties of CB molecules with different CSLs will be compared in the aim to explore the effect of CSL.

2. SIMULATION DETAILS

2.1. Quantum Chemical Calculations. Quantum chemical (QC) calculations were carried out using Gaussian09.[24] For each CB molecule, we rotated the dihedral angles C(N)−N−C−C and C−C−C−O to generate the input conformations for quantum chemical calculations. All of the conformations were first minimized with a classical UFF force field[25] and then further optimized in an implicit water solvent at the B3LYP/6-311++G(d,p) level. The polarizable continuum model was used to describe the implicit water solvent.[26] The optimized conformations were used for the calculation of partial charge and analysis of electrostatic potential surface and the electron density. For each CB molecule, the conformation with the lowest potential energy was chosen for single-point calculation for the analysis of electrostatic potential surface.

In this work, a new set of partial charges were calculated for each CB molecule with quantum chemical calculation. The atomic charges of the CB molecules were calculated with the CHELP algorithm,[27] which fits the atomic charges to the electrostatic potential of the molecule. For each CB molecule, the atomic partial charges used in MD simulations were obtained by averaging in two steps. The first is the average among the same type of atoms in one single conformation. In one CB molecule, the same type of atoms means all the atoms in the same geometrical and chemical positions, such as the nine hydrogen atoms of the three methyl groups bonding to the nitrogen atom. The second is the average among various conformations weighted by the Boltzmann factor. The force field parameters of all five CB molecules were listed in Tables S1−S4, Supporting Information.

2.2. Molecular Dynamics Simulations. The schematics of the five CB molecules are shown in Figure 1. All-atom models are used in this work. The SPC/E water model[28] was used because of its good representation of the dipole moment, dielectric constant, and diffusion properties of water molecules. The potential energy of intermolecular interactions is calculated as a combination of a Lennard-Jones (L-J) 12−6 potential and a Coulomb potential, as shown in eq 1.

$$U(r_{ij}) = 4\varepsilon_{ij}\left[\left(\frac{\sigma_{ij}}{r_{ij}}\right)^{12} - \left(\frac{\sigma_{ij}}{r_{ij}}\right)^{6}\right] + \frac{q_i q_j}{r_{ij}} \quad (1)$$

where r_{ij} is the distance between atoms i and j, q_i is the partial charge assigned to atom i, and ε_{ij} and σ_{ij} are energy and size parameters obtained by Jorgensen combining rules.

The L-J parameters were obtained from the OPLS all-atom (OPLSAA) force field[29] developed by the Jorgensen group because of its good representation of small organic molecules. The details for the calculation of partial charges were described in Section 2.1. Table S1 (Supporting Information) lists the L-J parameters and partial charges for the five CB molecules used in this work. The parameters for intramolecular interactions, including bond, angle, and dihedral interactions, were also derived from the OPLSAA force field.

The simulation system for the investigation of hydration was a periodic water box containing water molecules and one CB molecule. The molecular dynamics (MD) simulations were performed using Gromacs (version 4.5.4)[30] in an isobaric−isothermal ensemble (NPT). For all the five CB cases, after energy minimization and a 1.0 ns MD run with an integral step of 1.0 fs for equilibrium, another 1.0 ns run was carried out with an integral step of 2.0 fs. The coordinates were saved every 0.2 ps. Long-range electrostatic interactions were computed with the particle mesh Ewald method with periodic boundary conditions in all three dimensions.[31] The short-range van der Waals interactions were calculated with a cutoff distance of 1.1 nm. During the first 1.0 ns MD run for equilibrium, the system was maintained at 298 K (0.1 ps time constant) and 100.0 kPa with the Berendsen algorithm[32] (with a compressibility of 4.5×10^{-5} bar^{-1} and a 1 ps time constant). During the second 1.0 ns MD simulation for data collection, the system was maintained at 298 K with the Nose−Hoover algorithm[33,34] and 100 kPa with the Parrinello−Rahman algorithm.[35] Intramolecular bonds of betaine molecules and water molecules were kept constrained with the LINCS algorithm.[36] MD simulations with the developed partial charges and the original ones from the OPLSAA force field were performed and compared.

In order to compare the force fields with partial charges developed in this work and from the OPLSAA force field, we also calculated the interaction energy E of the CB molecule and one water molecule from QC calculations and with these two sets of force fields, as listed in Table S5, Supporting Information. The initial conformations of the five CB−water systems were shown in Figure S2, Supporting Information. The result of CB0 with partial charges developed in this work is much closer to that from QC calculations than that with partial charges from the OPLSAA force field. In addition, E values for the CB molecules with longer CSL are lower than those for the CB molecules with shorter CSL. This indicates the variation of the partial charges of those CB molecules with CSL and the necessity to recalculate their partial charges, especially to those with shorter CSL in which charge transfer occurs.

For the five CB−Na^+ simulation cases, a 10.0 ns MD simulation was carried out for data collection after energy minimization and a 10.0 ns MD run for equilibrium. The simulation system was the same as that used in our previous work.[21] The other details were the same as in the CB cases.

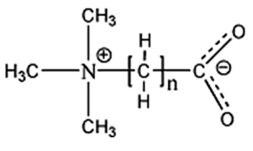

Figure 1. Chemical structure of CB_n molecules (n = 0, 1, 2, 3, and 4).

dx.doi.org/10.1021/jp3094534 | J. Phys. Chem. B 2013, 117, 1357−1366

2.3. Metadynamics Calculations for Na^+ Association Free Energy. The metadynamics algorithm developed by Laio et al.[37] was used to evaluate the association free energy of Na^+ and CB molecules. We applied a well-tempered metadynamics simulation[38] since it rescales the Gaussian weight factor and guarantees the convergence of simulation. The two selected collective variables were the distances between Na^+ and the two oxygen atoms of CB molecule. The initial Gaussian weight factor was set to be 1.5 kJ·mol^{-1}, and the deposition rate of the Gaussian bias terms was set to be 250 fs with a bias factor of 10. The standard deviation for the Gaussian bias term was set to be 0.05. The whole simulation time is 100 ns, and the output frequency is 250 fs. All the metadynamics simulations were carried out in a NVT ensemble with v-rescale algorithm[39] to control the temperature around 298 K using Plumed-1.3.0[40] implemented gromacs-4.5.5.

3. RESULTS AND DISCUSSIONS

3.1. Electrostatic Potential Surfaces of CB Molecules. Partial charges of the two charged groups are critical to the hydration and ionic association of a zwitterion. Variation of the CSL changes their distance and affects the charges. Figure 2 shows the electrostatic potential surfaces (EPSs) of the most optimized structure of the five CB molecules in implicit water solvent. It can be seen that the EPS color of carboxylic groups of CB0 and CB1 is considerably lighter than the others. The same phenomenon is observed in the color depths of EPS around trimethyl ammonium groups. This observation indicates that the two charged groups in CB0 and CB1 are both less charged than their counterparts in CB molecules with longer CSLs, due to the strong interplay between them.

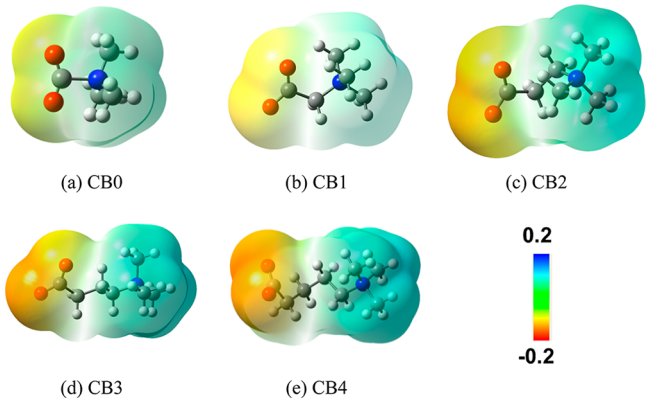

Figure 2. EPSs of (a) CB0, (b) CB1, (c) CB2, (d) CB3, and (e) CB4.

In CB molecules with longer CSLs, the interplay between charged groups decreases sharply. As shown in Figure 2, the color depths of corresponding EPSs around charged groups are similar in CB3 and CB4. This similarity indicates that variation of the CSL cannot affect the interplay between charged groups as significantly as in CB molecules with shorter CSLs. This is expected because the two charged groups must be very close to interplay with each other. The distance increase induced by growing CS weakens this interplay sharply. It has been reported[7] that the pK_a of a CB1 surfactant is around 2, lower than that of CB2 surfactant (around 3.2), which is consistent with the sharp decrease in interplay observed in this work. Thus, we may expect that, when the CSL < 3, the variation of CSL may affect the hydration and ionic association significantly. When CSL ≥ 3, the variation of CSL may just tune the number of methylene groups in the molecule and molecular flexibility, but hardly change the partial charges of two charged groups.

We further analyzed the electron distributions around the carboxylic groups of the five conformations shown in Figure 2 using Bader analysis.[41,42] Different from CHELP algorithm, Bader analysis calculates the atomic charge based on the number of electrons near the atom. In Bader analysis, the whole space of electrons is divided into Bader regions by the zero flux surfaces. A zero flux is a 2-D surface on which the electron density is at a minimum perpendicular to the surface. The aim of this analysis is to observe whether the partial charges obtained from electron densities and calculated from the CHELP algorithm have similar tendency as CSL varies. As shown in Table 1, the partial charges calculated with these two methods showed the same trend with the variation of CSL, though their values are different. The carboxylic group in CB0 is much less negatively charged as compared to those in the CB molecules with longer CSL. Increasing CSL results in the enhancement of the negative charges of the carboxylic group, but this effect decreases as the CSL increases. The carboxylic groups in CB3 and CB4 have similar partial charges.

Table 1. Partial Charges of the Carboxylic Groups of the Five CB Molecules Obtained with Bader Analysis and CHELP Algorithm

	CB0	CB1	CB2	CB3	CB4
Bader(e)	−0.388	−0.822	−0.917	−0.964	−0.938
CHELP(e)	−0.494	−0.775	−0.844	−0.866	−0.868

3.2. Radial Distribution Functions between Water and CB Molecules. Hydration is recognized to be critically important to assess a zwitterion thoroughly.[3] To evaluate the hydration of a CB molecule properly, we first analyzed the radial distribution functions (RDFs) of water molecules and selected atoms of CB molecules. We selected the oxygen atoms of the carboxylic group, carbon atoms of the trimethyl ammonium group, and carbon atoms in the CS part as the feature atoms of these three parts. Figure 3 shows the RDFs of these atoms and oxygen atoms of the water molecules for MD simulations with the partial charges developed in this work and from the OPLSAA force field.

A peak in a RDF profile indicates the existence of a coordination shell, and its position defines the geometric radius of the coordination shell. As shown in Figure 3, both the RDFs with partial charges in this work and those from the OPLSAA force field show that only the O−Ow RDFs have obvious peaks, whereas no significant peaks can be observed for the other two RDFs. This difference in RDFs indicates the difference in the hydration of the carboxylic group and other parts of the molecule, and these two sets of force field parameters give consistent results. To O−Ow RDFs, we observe that their peaks in Figure 3a1 and Figure 3a2 are at the same positions. These two sets of force field parameters give the same results on the size of the coordination shell of the carboxylic group.

With the partial charges in this work, the peaks of O−Ow RDFs show a variation as a function of CSL similar to that observed for EPS color depth. As shown in Figure 3a1, the peak height for CB0 is 1.5 and increases to 3.0 for CB1. The peak heights for CB3 and CB4 are higher than the ones of CB1 and CB0 and very similar to each other. This indicates that the

dx.doi.org/10.1021/jp3094534 | J. Phys. Chem. B 2013, 117, 1357−1366

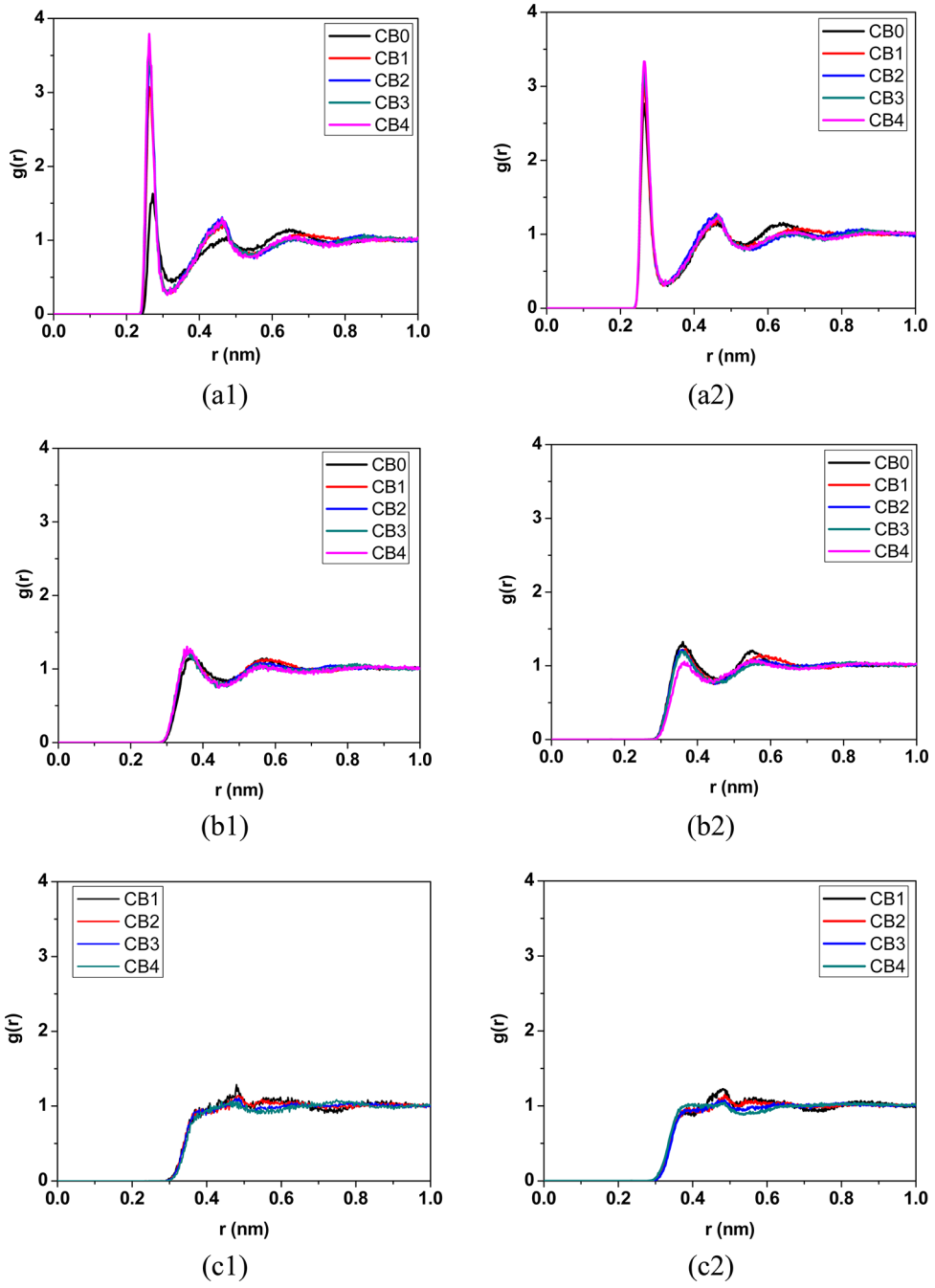

Figure 3. RDFs of atoms of CB molecules and oxygen atoms of water molecules in simulations with partial charges developed in this work or from the OPLSAA force field. (a1) O−Ow (this work), (a2) O−Ow (OPLSAA), (b1) C(N)−Ow (this work), (b2) C(N)−Ow (OPLSAA), (c1) C(C)−Ow (this work), and (c2) C(C)−Ow (OPLSAA).

hydration of the carboxylic group may show variation in CB molecules with shorter CSLs and be similar in those with CSL $\geq$ 3. For the other parts of the molecule, we can observe that C(N)−Ow and C(C)−Ow RDFs merely change as the CSL varies, indicating that their hydration may not show a significant change as the CSL varies. In the OPLSAA force field, the carboxylic groups in five CB molecules are set to have the same partial charges, and there is no significant variation in peak height, as shown in Figure 3a2.

3.3. Coordination Numbers. A previous study has shown that water molecules in the coordination shells of trimethyl ammonium and carboxylic groups have significantly different structures and dynamics.[43] When close enough, the two coordination shells may overlap geometrically and affect the behavior of water molecules in the shells. We investigated the overlap phenomenon by analyzing the numbers of water molecules in the overlap region of the coordination shells of the two charged groups and only in the shells of the charged groups. The coordination shells of these two charged groups are defined in the same way as in our previous work[43] based on the RDFs shown in Figure 3. Table 2 lists the numbers of water molecules in the overlap (in the shells of both carboxylic and trimethyl ammonium groups), negative (only in the shell of carboxylic group), positive (only in the shell of trimethyl ammonium group), and CS (only in the shell of CS part) regions, as well as the number of water molecules in these

dx.doi.org/10.1021/jp3094534 | J. Phys. Chem. B 2013, 117, 1357−1366

Table 2. Number of Water Molecules in Positive, Negative, CS and Overlap Regions and Their Sum

		positive	negative	CS	overlap	sum
CB0	this work	17.10	2.91	0.00	2.26	22.27
	OPLSAA	17.70	4.46	0.00	2.58	24.74
CB1	this work	17.35	5.56	2.63	1.61	27.15
	OPLSAA	17.67	6.21	2.96	1.39	28.23
CB2	this work	18.06	6.62	4.31	0.76	29.75
	OPLSAA	17.40	5.21	3.86	1.34	27.81
CB3	this work	17.85	6.25	7.34	0.98	32.42
	OPLSAA	20.23	4.83	6.03	1.26	32.35
CB4	this work	18.60	6.76	9.44	0.50	35.30
	OPLSAA	16.09	6.62	11.86	0.74	35.31

regions obtained from MD simulations with partial charges developed in this work and from the OPLSAA force field.

As listed in Table 2, the numbers of water molecules in the four regions from MD simulations with partial charges developed in this work are similar to those from simulations with partial charges from the OPLSAA force field. Therefore, the effect of CSL will be analyzed only based on the simulation results with partial charges developed in this work. For CB0, the numbers of water molecules in the negative and overlap regions are 2.91 and 2.26, respectively, which means that around 44% of water molecules in the coordination shell of the carboxylic group are also considered in the shell of the trimethyl ammonium group. This significant overlap indicates that the water molecules in the coordination shell of the carboxylic group of CB0 have structure and dynamics differently from those CB molecules with longer CSs. This overlap decreases rapidly as the CSL increases. For instance, for CB1, the numbers for the overlap and negative regions are 1.61 and 5.56. This means that the percentage decreases from 44% to only 23%. For CB molecules with a CSL $\geq$ 2, the number for the overlap region decreases to less than one, indicating that the overlap may be not even a stable phenomenon.

To the water molecules in the coordination shell of trimethyl ammonium groups, the effect of overlap may be weaker since the coordination number for the trimethyl ammonium group is definitively larger than the corresponding number for the carboxylic group. As listed in Table 2, the water molecules in the overlap region only count for at most 12% of all the water molecules in the coordination shell of the trimethyl ammonium group. However, since the effect of the carboxylic group on a water molecule is profoundly stronger than the that of the trimethyl ammonium group,[43] it is not clear up to now about how the water molecules in the coordination shell of the positively charged group would vary because of this overlap. Further investigation of the hydration structure and dynamics is necessary to offer a clear view.

The number for the CS region increases monotonically with the growing CSL, as listed in Table 2. The previous RDFs in Figures 3c1 and 3c2 have indicated that the water molecules of this region behave like those near a nonpolar substance. Thus, this increase implies that there is more hydrophobic part in the hydration of the molecule.

3.4. Hydration Structures and Dynamics of CB Molecules. Besides the number of water molecules, their

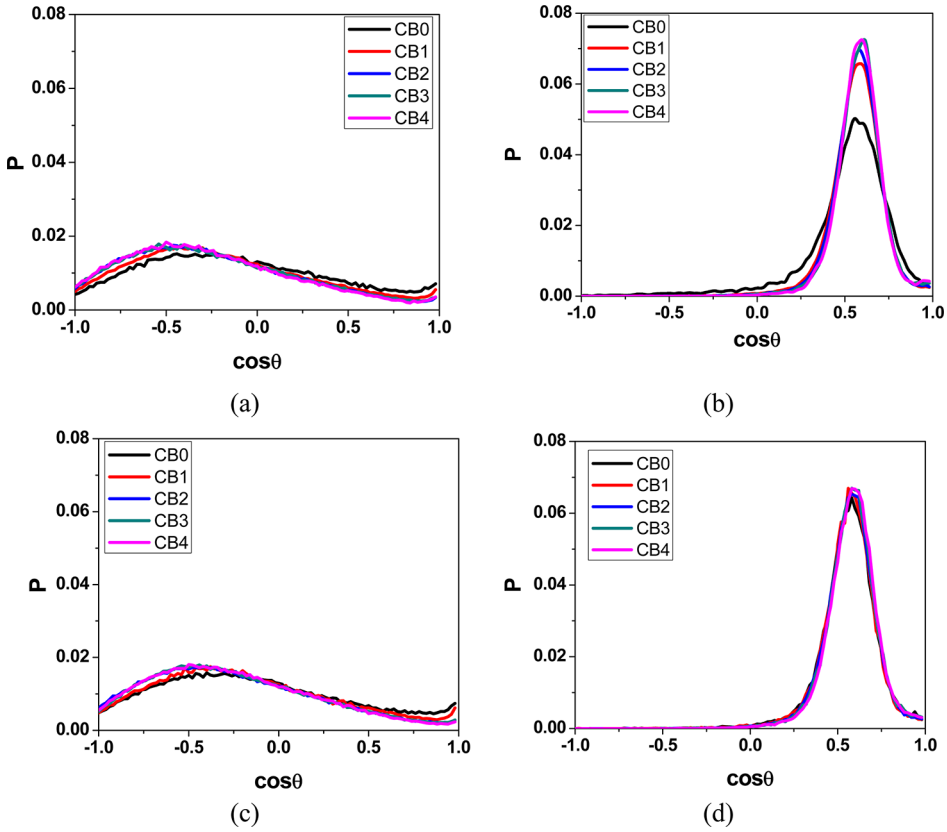

Figure 4. Distributions of cos θ for the dipole moment of water molecules in the coordination shells of trimethyl ammonium and carboxylic groups with partial charges developed in this work and from the OPLSAA force field. (a) Trimethyl ammonium and (b) carboxylic groups with partial charges from this work; (c) trimethyl ammonium and (d) carboxylic groups with partial charges from the OPLSAA force field.

dx.doi.org/10.1021/jp3094534 | J. Phys. Chem. B 2013, 117, 1357−1366

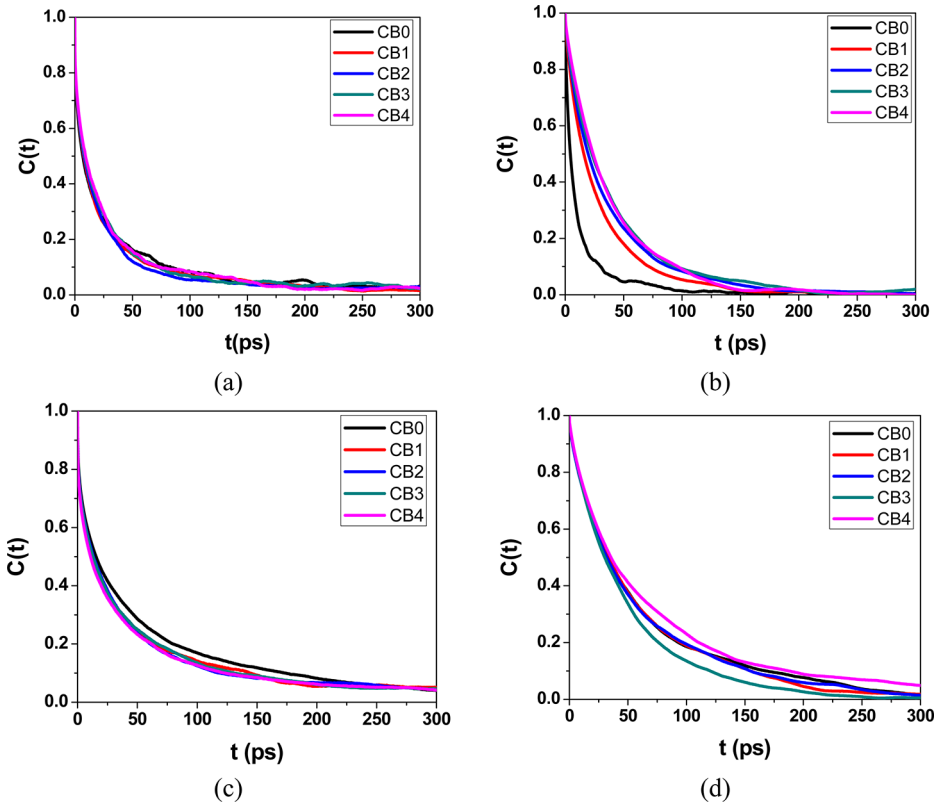

Figure 5. Residence time curves $C(t)$ of water molecules in the coordination shells of trimethyl ammonium and carboxylic groups with partial charges developed in this work and from the OPLSAA force field. (a) Trimethyl ammonium and (b) carboxylic groups with partial charges from this work; (c) trimethyl ammonium and (d) carboxylic groups with partial charges from the OPLSAA force field.

structure[43,44] and dynamics[43] are also critically important to evaluate the molecular hydration thoroughly. The hydration structure and dynamics of carboxylic and trimethyl ammonium groups were investigated by analyzing the distributions of dipole orientation θ and residence curve $C(t)$ of water molecules in the respective coordination shells of charged groups, as defined in our previous study.[43] The water molecules in the overlap region are considered to be in the coordination shells of both charged groups. Figure 4 shows the distributions of cosθ of the coordination shells of the two charged groups with partial charges developed in this work (Figure 4a,b) and from the OPLSAA force field (Figure 4c,d). Figure 5 shows $C(t)$ of the coordination shells of the two charged groups with partial charges developed in this work (Figure 5a,b) and from the OPLSAA force field (Figure 5c,d).

As shown in Figure 4, the distributions of cosθ for the carboxylic group from simulations with partial charges developed in this work and from the OPLSAA force field present different variations as to the variation in the CSL. The distribution with partial charges developed in this work has its peak height increase when the CSL increases. The peak height remains identical when the CSL $\geq$ 3. This indicates that the hydration structure of the carboxylic group increases as the CSL increases and reaches a steady state when CSL $\geq$ 3. The distribution from simulations with partial charges from the OPLSAA force field does not present the similar variation. Instead, the distributions for all five CB molecules are nearly identical, as shown in Figure 4d. This indicates that the hydration structures of the carboxylic groups of all five CB molecules are similar. The simulation results with both of these two sets of partial charges show that the distribution of cosθ for the trimethyl ammonium group does not have a significant variation as the CSL varies.

The analysis of $C(t)$ reveals the tendency for water molecules to stay near the carboxylic group. The respective residence times τ for the five curves in Figure 5b, calculated with the same method as in our previous paper,[43] are 8.64 ps (CB0), 27.06 ps (CB1), 33.54 ps (CB2), 37.28 ps (CB3), and 37.01 ps (CB4). The increment ratios are 213% (CB0−CB1), 24% (CB1−CB2), 11% (CB2−CB3), and −1% (CB3−CB4). This indicates that water molecules stay in the coordination shell of the carboxylic group longer as the CSL increases, and this increase only occurs when the CSL < 3. When the CSL $\geq$ 3, the CSL variation will not change the residence time of water molecules near the carboxylic group. τ for the five curves in Figure 5d are 56.58 ps (CB0), 55.92 ps (CB1), 55.69 ps (CB2), 46.83 ps (CB3), and 65.00 ps (CB4). This indicates that, with partial charges from the OPLSAA force field, there is no CSL dependence for τ.

Experiments have shown that the CB molecule with a shorter CSL has a lower pK_a. The lower pK_a indicates that the carboxylic group in a CB molecule with a shorter CSL has a weaker ability to attract hydrogen atoms. Therefore, the interaction between the carboxylic group and water molecules should be weaker for a CB molecule with a shorter CSL. The results from MD simulations with partial charges developed in this work show a CSL dependence consistent with that trend in pK_a measurements, while the simulations with partial charges from the OPLSAA force field does not show such variation.

As the CSL increases, the carboxylic group is becoming more highly charged, and the overlap with the coordination shell of the trimethyl ammonium group is decreasing. The interaction

dx.doi.org/10.1021/jp3094534 | J. Phys. Chem. B 2013, 117, 1357−1366

between water molecules and the carboxylic group is growing stronger, and the behavior of water molecules is more determined by the carboxylic group only. Consequently, the hydration structure and dynamics increases. When CSL ≥ 3, variation of the CSL cannot cause significant variation of partial charges in the carboxylic group and the overlap. Thus, the cos θ distribution and $C(t)$ are nearly identical.

3.5. Hydration Free Energy of CB Molecules. Hydration free energy ΔG is used in the aim to describe the hydration of the whole molecule as a function of CSL. The hydration free energy was calculated using the perturbation method as in our previous study.[43] We only studied ΔG with partial charges developed in this work because the results with them are consistent with the observations from experimental pK_a measurements. In addition to the five CB molecules with CSLs ranging from one to four, we added three more CB molecules with CSLs of six, eight, and ten methylene groups to investigate the effect of the CSL on hydration free energy on a larger scale. For the three newly added CB molecules, the partial charges of atoms in their charged groups are the same as the ones of the CB4 molecule, and the additional methylene groups are parametrized with the OPLSAA force field. Figure 6 shows the relative hydration free energy ($\Delta\Delta G$) of these eight CB molecules as a function of CSL with the average hydration free energy of CB3 taken as a reference.

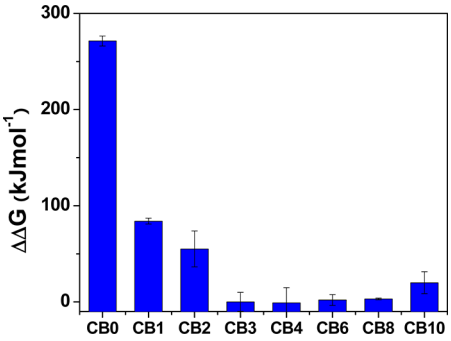

Figure 6. Relative hydration free energy ($\Delta\Delta G$) of CB molecules as a function of CSL.

The hydration free energy of CB0 is the highest among these eight CB molecules. For CB molecules with CSL < 3, the increase of CSL results in a decrease of $\Delta\Delta G$. This is attributed to the charge increase of the two charged groups. However, the reduction rate decreases as CSL increases. For instance, the hydration free energy of CB1 is nearly 170 kJ·mol^{-1} lower than that of CB0, while the hydration free energy of CB2 is only around 30 kJ·mol^{-1} lower than that of CB1. The hydration free energy is related to the hydration structure and dynamics around the overall molecule. For CB molecules with shorter CSLs, the main contributor to the variation of hydration free energy is the hydration of the two charged groups. As shown in the previous analysis, from CB0 to CB1, the hydration structure and dynamics around the carboxylic group exhibits the most significant change. With the increase in the CSL, the variation rate of the hydration structure and dynamics in regards to the CSL decreases. Consequently, the variation rate of the hydration free energy decreases.

We cannot observe significant variation of the hydration free energy for those CB molecules with CSL ≥ 3. As we have shown in previous sections, the trimethyl ammonium and carboxylic groups in these molecules have similar hydration structure and dynamics. Thus, the main contributor to the variation of hydration free energy for these CB molecules may come from the CS part itself. The methylene group is hydrophobic and supposed to increase the hydration free energy. However, the change of hydration free energy brought by the methylene group is small. For instance, the hydration free energy of ethane is 11.0 kJ·mol^{-1}, while the value for propane is 12.1 kJ·mol^{-1},[45] indicating that the addition of one methylene group may just add around 1.1 kJ·mol^{-1} to the hydration free energy; this is not very noticeable compared to that caused by the charge variation of the two charged groups.

3.6. Association of Na^+ with CB molecules. Na^+ is ubiquitous in nature and associates with the carboxylic group of CB molecules. The association can vary with CSL since the variation of CSL results in the change of electron density for the carboxylic group. In this work, Na^+−CB associations were analyzed from structure, dynamics, and energy aspects. The association is also only studied with partial charges developed in this work because these results are consistent with the observations from experimental pK_a measurements. The association structure was investigated with RDF between Na^+ and oxygen atoms of the CB molecule, as shown in Figure 7a. All five profiles present a significant peak at a position of around 0.25 nm, demonstrating that Na^+ can form a stable and direct association with the oxygen atoms of all of them. The peak height varies significantly with the CSL. As shown in Figure 8a, the peak height follows the sequence: CB0 < CB1 <

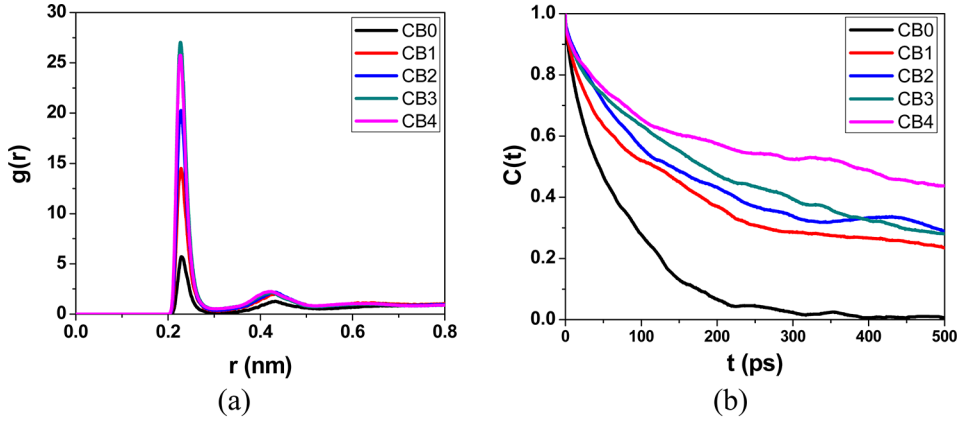

Figure 7. Na^+−CB associations: (a) RDFs and (b) residence curves of association of Na^+ and oxygen atoms of CB molecules.

dx.doi.org/10.1021/jp3094534 | J. Phys. Chem. B 2013, 117, 1357−1366

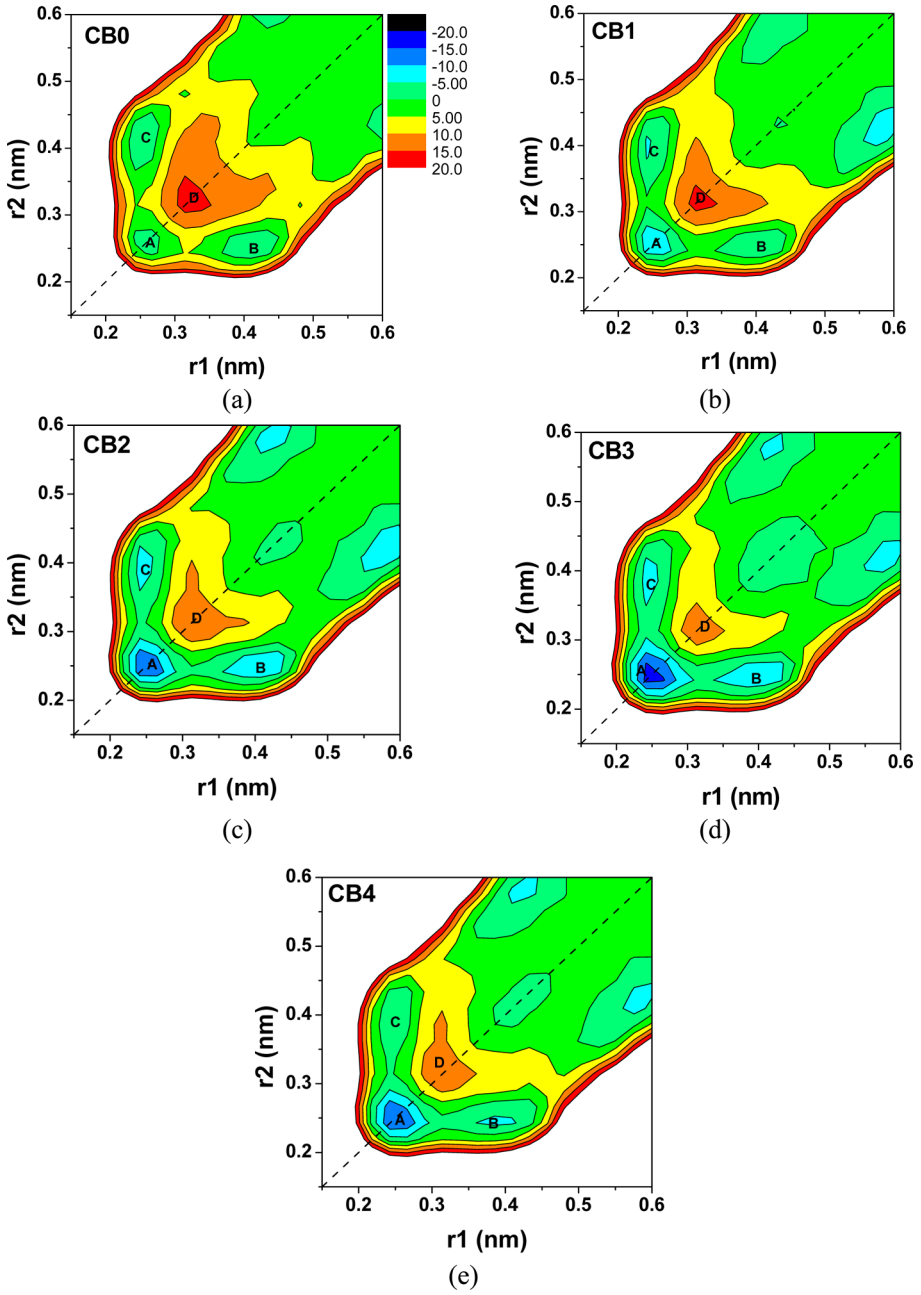

Figure 8. Association free energy of five CB molecules with Na^+: (a) CB0–Na^+, (b) CB1–Na^+, (c) CB2–Na^+, (d) CB3–Na^+, and (e) CB4–Na^+. r1 and r2 are the distances between Na^+ and the two oxygen atoms of CB molecules.

CB2 < CB3 ≈ CB4. The peak heights of CB3 and CB4 are nearly five times that of CB0. Such considerable difference indicates that CB molecules with longer CSLs may have a much higher preference to associate with Na^+, due to the higher partial charges of their carboxylic group. This tendency is further confirmed by the analysis of association dynamics. As shown in Figure 7b, the association residence curve for the CB molecule with a long CSL decays slower than the ones of short CSL, indicating a stronger and more stable association.

Figure 8 shows the free energy contour plots as a function of distance between Na^+ and two oxygen atoms of CB molecule, r_1 and r_2. For every contour plot, we can observe three minimum regions labeled as A, B, and C in each figure. These three minimum regions correspond to two types of associations between Na^+ and CB molecules. As shown in Figure 8, region A has both r_1 and r_2 in the scale from 0.23 to 0.27 nm, close to the peak position (0.25 nm) observed in the RDFs. This represents the situation that Na^+ associates with both oxygen atoms. Regions B and C has either r_1 or r_2 close to 0.25 nm, and the other collect variables in the scale from 0.35 to 0.45 nm. These two regions represent the situation that Na^+ only associates with one oxygen atom.

The formation of a direct association needs to overcome an energy barrier sourced from the depletion and rearrangement of a certain part of coordination shells of both solutes. As shown in Figure 8, for every CB molecule, we can observe a plateau that represents the energy barrier. We can find that the maximum energy barriers for CB0 and CB1 are higher than 15 $kJ \cdot mol^{-1}$, whereas the corresponding values for CB2, CB3, and CB4 are all less than 15 $kJ \cdot mol^{-1}$. In addition, we can observe

dx.doi.org/10.1021/jp3094534 | J. Phys. Chem. B 2013, 117, 1357–1366

that the barrier region with an energy higher than 10 kJ·mol^{-1} decreases with an increasing CSL. These two observations also indicate that the CB molecules with long CSLs more easily form associations with Na^+.

4. CONCLUSIONS

In this work, we investigated the effect of CSL on the properties of CB molecules using molecular simulations and quantum chemical calculations. Five CB molecules with CSLs ranging from zero to four were used. Their EPS, hydration, and association with Na^+ were studied and compared. The EPS analysis showed that the charged groups in CB molecules with a short CSL are less charged and that their charges are dependent on the CSL, while the corresponding groups in the CB molecules with a CSL $\geq$ 3 demonstrate nearly identical charges. Hydration of the five CB molecules was studied and compared using MD simulations with partial charges developed in this work and from the OPLSAA force field. Simulations with both sets of force field parameters show that the overlap of coordination shells of the trimethyl ammonium and carboxylic groups is only observed in CB0 and CB1, but they show different results for hydration structure and dynamics of the two charged groups. Simulation results with partial charges from the OPLSAA force field do not show a significant dependence on CSL because the partial charges of the charged groups for all the five CB molecules are set to be identical. However, simulation results with partial charges developed in this work show the determining effect of CSL, which is consistent with the observations from experimental pK_a measurements. Simulation results with partial charges in this work show that hydration of trimethyl ammonium and carboxylic groups have different behaviors in regards to the CSL variation. The hydration of the former does not vary as the CSL does, while the hydration of the latter becomes stronger as the CSL increases and is similar for the CB molecules with a CSL $\geq$ 3. The hydration free energy of CB molecules with a CSL < 3 has a strong dependence on the CSL, while those of CB molecules with a CSL $\geq$ 3 do not show significant variation. The analysis of the RDF, lifetime, and free energy of CB−Na^+ association also shows a strong dependence on the CSL, affirming its importance.

■ ASSOCIATED CONTENT

Supporting Information

Figure S1 shows the schematics of the five CB molecules. Figure S2 shows conformations for the five CB−water systems. Tables S1 shows the nonbond interaction parameters of atoms of the five CB molecules. Tables S2−S4 show the bond, angle, and torsion parameters of the five CB molecules. Table S5 shows the interaction energy E of one CB molecule and one water molecule for the five CB molecules calculated with QC calculations and classical force fields. This material is available free of charge via the Internet at http://pubs.acs.org.

■ AUTHOR INFORMATION

Corresponding Author

*E-mail: sjiang@u.washington.edu. Phone: 206-616-6509.

Notes

The authors declare no competing financial interest.

■ ACKNOWLEDGMENTS

This work was supposed by the Office of Naval Research (N00014-10-1-0600), the Defense Threat Reduction Agency (HDTRA1-10-1-0074), and the National Science Foundation (CBET-0854298). This research was also supported in part by the National Science Foundation through TeraGrid resources provided by NICS and TACC under grant number TG-CHE110006. This work was facilitated through the use of advanced computational, storage, and networking infrastructure provided by the Hyak supercomputer system, supported in part by the University of Washington eScience Institute.

■ REFERENCES

(1) Hanson, A. D.; Rathinasabapathi, B.; Rivoal, J.; Burnet, M.; Dillon, M. O.; Gage, D. A. *Proc. Natl. Acad. Sci. U.S.A.* **1994**, *91*, 306−310.
(2) Yancey, P. H. *J. Exp. Biol.* **2005**, *208*, 2819−2830.
(3) Cao, Z. Q.; Yu, Q. M.; Xue, H.; Cheng, G.; Jiang, S. Y. *Angew. Chem., Int. Ed.* **2010**, *49*, 3771−3776.
(4) Carr, L. R.; Krause, J. E.; Ella-Menye, J. R.; Jiang, S. Y. *Biomaterials* **2011**, *32*, 8456−8461.
(5) Keefe, A. J.; Jiang, S. *Nat. Chem.* **2012**, *4*, 59−63.
(6) Jiang, S. Y.; Cao, Z. Q. *Adv. Mater.* **2010**, *22*, 920−932.
(7) Weers, J. G.; Rathman, J. F.; Axe, F. U.; Crichlow, C. A.; Foland, L. D.; Scheuing, D. R.; Wiersema, R. J.; Zielske, A. G. *Langmuir* **1991**, *7*, 854−867.
(8) Zhou, T. H.; Zhao, J. X.; You, Y. *J. Dispersion Sci. Technol.* **2009**, *30*, 1135−1141.
(9) Zhang, Z.; Vaisocherova, H.; Cheng, G.; Yang, W.; Xue, H.; Jiang, S. Y. *Biomacromolecules* **2008**, *9*, 2686−2692.
(10) Vaisocherova, H.; Zhang, Z.; Yang, W.; Cao, Z.; Cheng, G.; Taylor, A. D.; Piliarik, M.; Homola, J.; Jiang, S. *Biosens. Bioelectron.* **2009**, *24*, 1924−1930.
(11) Mi, L.; Giarmarco, M. M.; Shao, Q.; Jiang, S. *Biomaterials* **2012**, *33*, 2001−2006.
(12) Abraham, S.; So, A.; Unsworth, L. D. *Biomacromolecules* **2011**, *12*, 3567−3580.
(13) Bohrisch, J.; Schimmel, T.; Engelhardt, H.; Jaeger, W. *Macromolecules* **2002**, *35*, 4143−4149.
(14) Favresse, P.; Laschewsky, A. *Macromol. Chem. Phys.* **1999**, *200*, 887−895.
(15) Delgado, C.; Merchan, M. D.; Velazquez, M. M.; Anaya, J. *Colloid Surf., A* **2006**, *280*, 17−22.
(16) MacDonald, A. M.; Sheppard, M. A. W.; Lucy, C. A. *Electrophoresis* **2005**, *26*, 4421−4428.
(17) Bagchi, B. *Chem. Rev.* **2005**, *105*, 3197−3219.
(18) Chen, S.; Li, L.; Zhao, C.; Zheng, J. *Polymer* **2010**, *51*, 5283−5293.
(19) Christenson, H. K.; Claesson, P. M. *Adv. Colloid Interface Sci.* **2001**, *91*, 391−436.
(20) Meyer, E. E.; Rosenberg, K. J.; Israelachvili, J. *Proc. Natl. Acad. Sci. U.S.A.* **2006**, *103*, 15739−15746.
(21) Shao, Q.; He, Y.; Jiang, S. Y. *J. Phys. Chem. B* **2011**, *115*, 8358−8363.
(22) He, Y.; Shao, Q.; Chen, S. F.; Jiang, S. Y. *J. Chem. Phys.* **2011**, *135*, 154702.
(23) Chen, M.; Briscoe, W. H.; Armes, S. P.; Klein, J. *Science* **2009**, *323*, 1698−1701.
(24) Frisch, M. J.; Trucks, G. W.; Schlegel, H. B.; Scuseria, G. E.; Robb, M. A.; Cheeseman, J. R.; Scalmani, G.; Barone, V.; Mennucci, B.; Petersson, G. A.; Nakatsuji, H.; Caricato, M.; Li, X.; Hratchian, H. P.; Izmaylov, A. F.; Bloino, J.; Zheng, G.; Sonnenberg, J. L.; Hada, M.; Ehara, M.; Toyota, K.; Fukuda, R.; Hasegawa, J.; Ishida, M.; Nakajima, T.; Honda, Y.; Kitao, O.; Nakai, H.; Vreven, T.; Montgomery, J. A., Jr.; Peralta, J. E.; Ogliaro, F.; Bearpark, M.; Heyd, J. J.; Brothers, E.; Kudin, K. N.; Staroverov, V. N.; Kobayashi, R.; Normand, J.; Raghavachari, K.; Rendell, A.; Burant, J. C.; Iyengar, S. S.; Tomasi, J.; Cossi, M.; Rega,

N.; Millam, J. M.; Klene, M.; Knox, J. E.; Cross, J. B.; Bakken, V.; Adamo, C.; Jaramillo, J.; Gomperts, R.; Stratmann, R. E.; Yazyev, O.; Austin, A. J.; Cammi, R.; Pomelli, C.; Ochterski, J. W.; Martin, R. L.; Morokuma, K.; Zakrzewski, V. G.; Voth, G. A.; Salvador, P.; Dannenberg, J. J.; Dapprich, S.; Daniels, A. D.; Farkas, O.; Foresman, J. B.; Ortiz, J. V.; Cioslowski, J.; Fox, D. J. *Gaussian 09*, revision A.01; Gaussian, Inc.: Wallingford, CT, 2009.
(25) Rappe, A. K.; Casewit, C. J.; Colwell, K. S.; Goddard, W. A.; Skiff, W. M. *J. Am. Chem. Soc.* **1992**, *114*, 10024−10035.
(26) Miertuš, S.; Scrocco, E.; Tomasi, J. *Chem. Phys.* **1981**, *55*, 117−129.
(27) Chirlian, L. E.; Francl, M. M. *J. Comput. Chem.* **1987**, *8*, 894−905.
(28) Berendsen, H. J. C.; Grigera, J. R.; Straatsma, T. P. *J. Phys. Chem.* **1987**, *91*, 6269−6271.
(29) Jorgensen, W. L.; Maxwell, D. S.; TiradoRives, J. *J. Am. Chem. Soc.* **1996**, *118*, 11225−11236.
(30) Van der Spoel, D.; Lindahl, E.; Hess, B.; Groenhof, G.; Mark, A. E.; Berendsen, H. J. C. *J. Comput. Chem.* **2005**, *26*, 1701−1718.
(31) Essmann, U.; Perera, L.; Berkowitz, M. L.; Darden, T.; Lee, H.; Pedersen, L. G. *J. Chem. Phys.* **1995**, *103*, 8577−8593.
(32) Berendsen, H. J. C.; Postma, J. P. M.; Vangunsteren, W. F.; Dinola, A.; Haak, J. R. *J. Chem. Phys.* **1984**, *81*, 3684−3690.
(33) Nose, S. *J. Chem. Phys.* **1984**, *81*, 511−519.
(34) Hoover, W. G. *Phys. Rev. A* **1985**, *31*, 1695−1697.
(35) Parrinello, M.; Rahman, A. *J. Appl. Phys.* **1981**, *52*, 7182−7190.
(36) Hess, B. *J. Chem. Theory Comput.* **2008**, *4*, 116−122.
(37) Laio, A.; Parrinello, M. *Proc. Natl. Acad. Sci. U.S.A.* **2002**, *99*, 12562−12566.
(38) Barducci, A.; Bussi, G.; Parrinello, M. *Phys. Rev. Lett.* **2008**, *100*, 020603.
(39) Bussi, G.; Donadio, D.; Parrinello, M. *J. Chem. Phys.* **2007**, *126*, 014101.
(40) Bonomi, M.; Branduardi, D.; Bussi, G.; Camilloni, C.; Provasi, D.; Raiteri, P.; Donadio, D.; Marinelli, F.; Pietrucci, F.; Broglia, R. A.; Parrinello, M. *Comput. Phys. Commun.* **2009**, *180*, 1961−1972.
(41) Bader, R. *Atoms in Molecules: A Quantum Theory*; Oxford University Press: New York, 1990.
(42) Henkelman, G.; Arnaldsson, A.; Jonsson, H. *Comput. Mater. Sci.* **2006**, *36*, 354−360.
(43) Shao, Q.; He, Y.; White, A. D.; Jiang, S. Y. *J. Phys. Chem. B* **2010**, *114*, 16625−16631.
(44) Shao, Q.; Zhou, J.; Lu, L. H.; Lu, X. H.; Zhu, Y. D.; Jiang, S. Y. *Nano Lett.* **2009**, *9*, 989−994.
(45) Gallicchio, E.; Kubo, M. M.; Levy, R. M. *J. Phys. Chem. B* **2000**, *104*, 6271−6285.